



Pore expansion of highly monodisperse phenylene-bridged organosilica spheres for chromatographic application

Yongping Zhang, Yu Jin, Hui Yu, Peichun Dai, Yanxiong Ke^{**}, Xinmiao Liang^{*}

School of Pharmacy, Engineering Research Center of Pharmaceutical Process Chemistry, Ministry of Education, East China University of Science and Technology, 130 Meilong Road, Shanghai 200237, China

ARTICLE INFO

Article history:

Received 8 December 2009

Received in revised form 10 January 2010

Accepted 13 January 2010

Available online 22 January 2010

Keywords:

Phenylene-bridged
Hybrid organosilica
Spheres
Pore expansion
HPLC

ABSTRACT

Monodisperse phenylene-bridged organosilica spheres show great potential as chromatographic stationary phase. In this paper, the tunable particle size of monodisperse phenylene-bridged organosilica spheres were prepared by co-condensing different proportion of 1,4-bis(triethoxysilyl)benzene (1,4-BTEB) and tetraethylorthosilicate (TEOS), and then pore size was expanded by two-step post-synthesis hydrothermal treatments using *N,N*-dimethyldecylamine (DMDA)/dodecylamine (DDA) and tris-(hydroxymethyl)-aminomethane (TRIS) in turn. Phenylene-bridged organosilica spheres with particle size of 3.0–3.5 μm and pore size of 85 Å were further surface modified by C_{18} group and tested in reversed-phase high performance liquid chromatography (RP-HPLC). The primary chromatographic results demonstrated that C_{18} bonded phenylene-bridged organosilica stationary phase has high retention and good chemical stability in the high pH mobile phase, which indicated that the phenylene-bridged organosilica can be used for HPLC packing supports.

© 2010 Elsevier B.V. All rights reserved.

1. Introduction

Silica particles are the most widely used packing materials for high performance liquid chromatography (HPLC). However, the stationary phases based on silica materials can normally being used in the mobile phase within the pH range between 2 and 8 due to their poor chemical stability [1–6]. At mobile phase pH value less than 2, the instability of the Si–O–Si bond leads to the loss of the stationary phase bonded to the silica [7]. At mobile phase pH value greater than 8, particle erosion will occur due to the dissolution of the silica particles, which can lead to the loss of column efficiency and the increase of column back pressure [8]. The column packed with polymers [9], graphitic carbon [10,11] or highly stable metal oxides (such as alumina [12], titania [13,14], and zirconia [13,15], etc.) can endure high-pH mobile phase. Unfortunately, these nonsiliceous packings suffer from other problems. For examples, organic polymers have low mechanical stability, while graphitic carbon and metal oxides exhibit strong adsorption of acid or base analytes due to the complicate surface properties, which will result in the difficulty of method development [16].

Recently, mesoporous organic/inorganic hybrid materials have attracted many research interests. A lot of mesoporous organosilica have been developed by condensing organosiloxanes with the

type of $(\text{R}'\text{O})_3\text{SiRSi}(\text{OR}')_3$ containing one bridge-group R [17–19], such as methane [20], ethylene [21,22], ethane [23,24] and phenylene [9,25–27] groups. On the surface of hybrid silicas, both organic group R and silanol groups exist. The former can be changed to tune the hydrophilicity/hydrophobicity properties of the hybrid silica surface. The later can be used to bond specific functional group through traditional synthesis procedure. Compared with silica material, the organic/inorganic hybrid materials exhibit excellent hydrothermal, chemical and mechanical stability [28,29]. These properties indicate that the column packed with such materials will be more durable under adverse conditions, which are highly desired for HPLC packings. For example, Waters cooperation have developed C_{18} HPLC stationary phase based on spherical methyl-hybrid particles [30,31] and ethyl-bridged hybrid silica particles [16], which are stable at a pH range of 1–12.

Phenylene-bridged hybrid organosilica is one of the most important classes of hybrid silica and has shown potential application in HPLC. In 2006, Fröba and co-workers first reported synthesis of spherical phenylene-bridged organosilicas with particle diameters between 3 and 15 μm [32]. Recently, we reported the synthesis of highly monodispersed phenylene-bridged hybrid organosilicas spheres with particle sizes of 2–3 μm , and their application in RP-HPLC [33]. However, the pore sizes of the phenylene-bridged hybrid organosilica in both reports can only reach 50–60 Å. The small pore size limits further surface modification by chemical bonding, which restricts their applications in the chromatographic separation. For the point of view, the silica chromatographic packing should have pore diameters exceeding 80 Å to provide high

^{*} Corresponding author. Tel.: +86 411 84379519; fax: +86 411 84379539.

^{**} Corresponding author. Tel.: +86 21 64250622; fax: +86 21 64250622.

E-mail addresses: key@ecust.edu.cn (Y. Ke), liangxm@ecust.edu.cn (X. Liang).

mass transfer [34–37]. In a continuation of this study, we now present the synthesis and pore size expansion of monodisperse phenylene-bridged hybrid organosilica. In this report, a two-step pore expansion method was developed to prepare the phenylene-bridged hybrid particle with suitable pore size for bonding. The chemical stability of the C18 bonded phenylene-bridged hybrid silica was evaluated to illustrate the advantage of phenylene-bridged hybrid silica.

2. Experimental

2.1. Chemicals

1,4-bis(Triethoxysilyl)benzene (1,4-BTEB) was purchased from Aldrich. *N,N*-dimethyldodecylamine (DMDA) was purchased from TCI. Dodecylamine (DDA), cetyltrimethylammonium bromide (CTAB) and tetraethylorthosilicate (TEOS) were purchased from Shanghai Chemical Reagent Inc. of Chinese Medicine Group. Other chemicals were commercially available and used as received.

2.2. Synthesis of monodisperse phenylene-bridged hybrid organosilica spheres

Phenylene-bridged organosilica was prepared using CTAB and DDA as a template according to the literature [33]. For the synthesis of PHS-1, DDA (6.67 g) and CTAB (0.67 g) were dissolved in a mixture of water/ethanol (350 mL/650 mL). Followed by addition of ammonia (0.8 mL) and the mixture of 1,4-BTEB (5.42 g, 12 mmol) and TEOS (23.4 g, 100 mmol), and then vigorously stirred for 1 min at 20 °C. After aged for 12 h in static condition at 20 °C, the precipitate were filtered out and washed by ethanol, then dried in air at room temperature.

The sample of PHS-2 was prepared following the same procedure, except that 1,4-BTEB (25.3 g, 56 mmol) and TEOS (13.1 g, 56 mmol) was used in the synthesis.

2.3. Pore expansion of PHS-1 and PHS-2 by swelling agent incorporation method (the SWE method).

In a typical procedure, 2 g product prepared in step 2.2 was dispersed in 40 mL of water emulsion containing 0.4 g of DDA and 2.0 g of DMDA. The mixture was transferred into a Teflon-coated autoclave, and then hydrothermally treated at 135 °C for 24 h. The product was filtered out and extracted twice with 150 mL ethanol containing 5.0 mL of 36% aqueous HCl solution. The materials were then filtrated out, washed by ethanol and dried in air. PHS-1 and PHS-2 were treated as this procedure to obtain product PHS-1a and PHS-2a, respectively.

2.4. Pore expansion of organosilica materials using TRIS as pore expander

1.5 g PHS-1a was dissolved in a solution of 0.4 g TRIS and 10 mL water, and then hydrothermally treated at 110 °C for 24 h. The product was filtered out and washed by water and methanol. This material was denoted as PHS-1b. Following this procedure, the product PHS-1c obtained from PHS-1a with treatment at 135 °C, PHS-2b and PHS-2c obtained from PHS-2a with treatment at 145 and 160 °C, respectively.

2.5. Surface modification of phenylene-bridged hybrid organosilicas by C₁₈

1.0 g PHS-2c was added to a three-necked round bottom flask equipped with a reflux condenser and inert gas inlet. The sample was dried in vacuum oven at 130 °C for 12 h. 15 mL dry

toluene, 0.8 mL pyridine and 2.0 g octadecyldimethylchlorosilane were added to the flask. The mixture was stirred at 110 °C for 24 h under N₂ atmosphere. 2.0 mL trimethylchlorosilane was added into the flask. The suspension was refluxed for another 12 h and cooled to room temperature. After filtration, the products were washed by toluene, dichloromethane and methanol. This material was denoted as PHS-C₁₈. For comparison, S-C₁₈ was synthesized with this procedure using commercial silica (particle size: 5 μm; pore diameter: 100 Å; surface area: 300 m²/g).

2.6. Material characterization.

X-ray powder diffraction (XRD) patterns were recorded on a Rigaku D/Max 2550 power diffraction system using Cu K α radiation. Nitrogen sorption experiments were performed on an ASAP2100 apparatus. The samples were dried at 150 °C under vacuum overnight prior to measurements. Surface areas and pore-size distribution were measured using the Brunauer–Emmett–Teller (BET) and Barrett–Joyner–Halenda (BJH) methods, respectively. Scanning electron micrographs (SEM) were obtained on a JSM-6360LV instrument. Elemental analysis was taken on a Vario EL III analyzer. The solid-state NMR spectra were recorded on a DSX 300 spectrometer (sample spinning frequency of 4.2 kHz; $\pi/2$ pulse width of 6 ms). ¹³C cross-polarization (CP) magic angle spinning (MAS) nuclear magnetic resonance (NMR) (¹³C CP-MAS NMR) spectra were obtained under the condition of a contact time of 1 ms, a recycle delay of 2 s and 1700 scans, and ²⁹Si CP-MAS NMR measured under the condition of a contact time of 5 ms, a recycle delay of 3 s and 880 scans.

HPLC evaluations were carried out using Agilent HPLC system, composed of an Agilent 1200 series, G1379B degasser, G1312B pump, G1367C Autosampler, and G1315C DAD. The materials PHS-2c, PHS-C₁₈, S-C₁₈ were dispersed into acetone and packed into stainless-steel column (50 mm × 2.1 mm I.D.) under 65 MPa with methanol by a slurry packing technique, respectively.

2.7. Column aging procedure

Alkaline (pH 10) column degradation studies were performed as following procedure: columns were exposed to a 50 mM triethylamine (TEA) solution (pH 10) for 60 min (0.2 mL/min, 50 °C), and then purged with water (0.2 mL/min, 50 °C) and acetonitrile (0.2 mL/min, 50 °C) for 10 min each. The efficiency of the column was tested using phenanthrene as solute and acetonitrile/H₂O (60/40, v/v) as the mobile phase. The flow rate was 0.2 mL/min. Column temperature was at 50 °C. UV detection was set at 254 nm. For unbonded PHS-2c column, acetonitrile/H₂O (30/70, v/v) was used as mobile phase.

3. Results and discussion

3.1. Synthesis of phenylene-bridged hybrid organosilica spheres

Previous studies have shown that the ratio of organic functional moiety and the silica precursor was one of the important factors affecting the morphology and pore size of the organosilicas materials [38–40]. Therefore, we investigated the influence of the 1,4-BTEB concentration on the morphology and pore size of phenylene-bridged organosilicas materials. Samples PHS-1 and PHS-2 are prepared by 1,4-BTEB/TEOS ratios of 1:10 and 1:1, respectively. The particle morphologies of the organosilica materials are shown by the scanning electron microscopy (SEM) images in Fig. 1. The two samples have well monodispersity and perfect spherical morphologies. Particle size of PHS-1 is at the range of 1.5–2.0 μm (Fig. 1(a)), while PHS-2 is at the range of 3.0–3.5 μm (Fig. 1(b)). The spheres sizes remarkably increased with the increasing amount

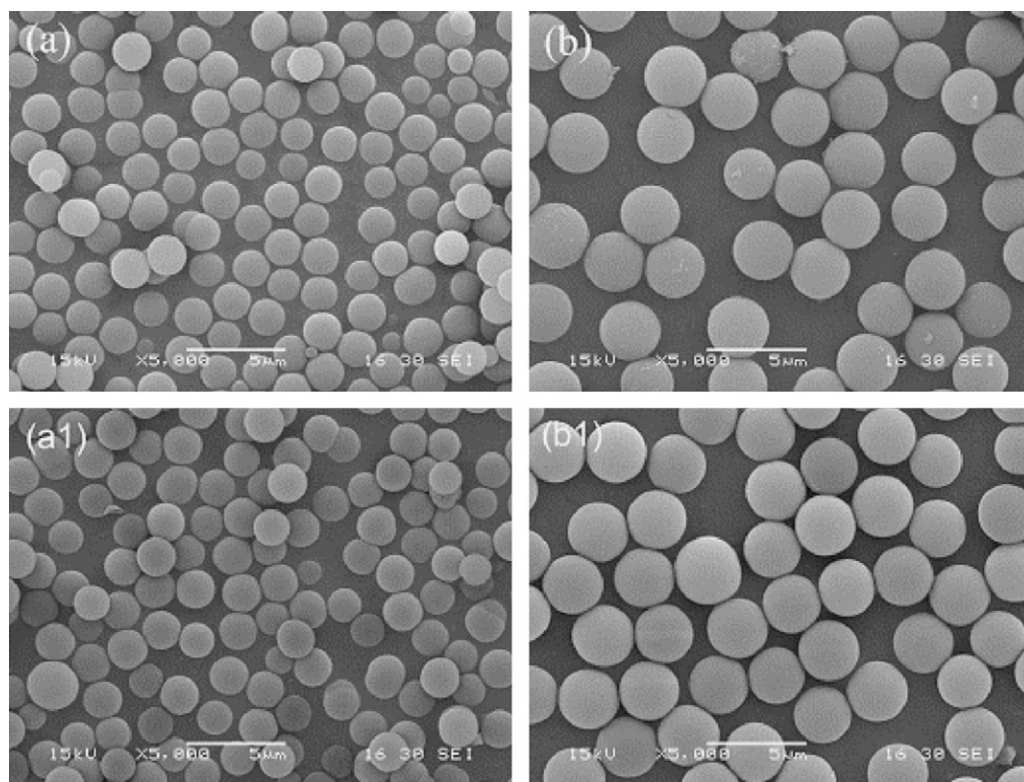


Fig. 1. SEM images of phenylene-bridged hybrid organosilica spheres of (a) sample PHS-1, (b) sample PHS-2, (a1) sample PHS-1c (hydrothermal treatment in TRIS solution at 135 °C); (b1) sample PHS-2c (hydrothermal treatment in TRIS solution at 160 °C).

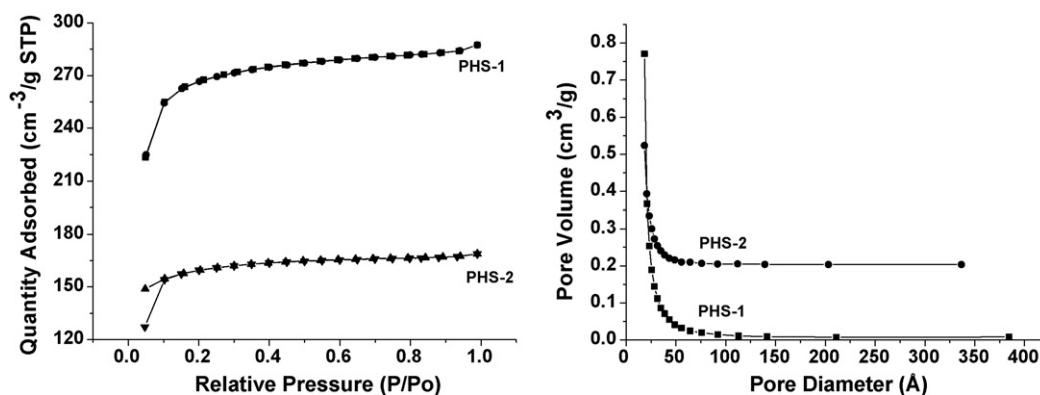


Fig. 2. N₂ adsorption–desorption isotherms and pore size distribution of samples PHS-1 (directly removed surfactants before hydrothermal treatment) and PHS-2 (directly removed surfactants before hydrothermal treatment).

of phenylene organic groups incorporated in the framework. It provides a way to produce the phenylene-bridged organosilica materials with a tunable particle size.

3.2. The pore sizes expansion of organosilica materials

Nitrogen adsorption–desorption isotherms and the corresponding BJH pore size distributions for materials PHS-1 and PHS-2 are shown in Fig. 2. All the materials exhibit the type I isotherms, suggesting that they are microporous materials, which is also proved by the pore size distributions curves. The detailed BET surface areas, total pore volumes and BJH pore diameters of the samples are listed in Table 1. Both of the samples of PHS-1 and PHS-2 have the pore size less than 18 Å before pore expansion. The sample of PHS-1 has the BET surface area of 818 m²/g and pore volume of 0.44 cm³/g, while the sample of PHS-2 has the BET surface area of 493 m²/g

Table 1
Structure parameters of each as-prepared sample.

Samples	Condition ^a	Pore size ^b (Å)	Surface area (m ² /g)	Pore volume (cm ³ /g)
PHS-1	(A)	<18	818	0.44
PHS-1a	(B)	40	564	0.70
PHS-1b	(C)	63	396	0.65
PHS-1c	(D)	100	193	0.48
PHS-2	(A)	<18	493	0.26
PHS-2a	(B)	35	835	0.66
PHS-2b	(E)	75	413	0.64
PHS-2c	(F)	85	354	0.63

^a Condition: (A) directly removed surfactants before hydrothermal treatment with DMDA and DDA; (B) removed surfactants after hydrothermal treatment with DMDA and DDA; (C) hydrothermal treatment in TRIS solution at 110 °C; (D) hydrothermal treatment in TRIS solution at 135 °C; (E) hydrothermal treatment in TRIS solution at 145 °C; (F) hydrothermal treatment in TRIS solution at 160 °C.

^b Pore sizes were calculated from desorption branch using BJH method.

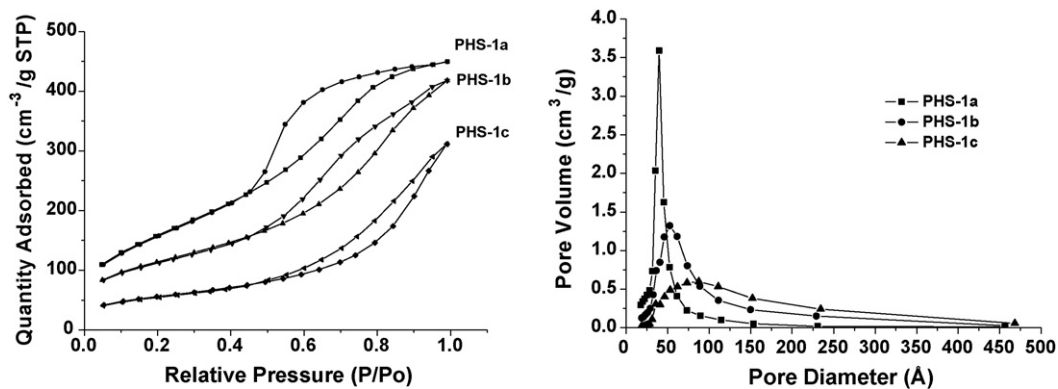


Fig. 3. N_2 adsorption–desorption isotherms and pore size distribution of PHS-1a (removed surfactants after hydrothermal treatment using DMDA at 135 °C), PHS-1b (after hydrothermal treatment using TRIS at 110 °C) and PHS-1c (after hydrothermal treatment using TRIS at 135 °C).

and pore volume of 0.26 cm^3/g . It can be observed that the surface area and pore volume decreased greatly when the ratio of 1,4-BTEB: TEOS increased.

In order to obtain phenylene-bridged hybrid materials with large pore size, the swelling method [41] and dissolution/redeposition technique [42] were used for the pore size expansion of as-prepared materials in this study. Nitrogen adsorption–desorption isotherms and the corresponding BJH pore size distributions for materials PHS-1 and PHS-2 after hydrothermal treatments are shown in Figs. 3 and 4, respectively.

After the hydrothermal treatment for 24 h using DMDA and DDA as swelling agents, the pore size and pore volume of PHS-1a were found increased to 40 Å and 0.70 cm^3/g , respectively. For the sample of PHS-2a, the same post-synthesis condition resulted in the increasing of pore size to 35 Å, and the pore volume to 0.66 cm^3/g . The nitrogen isotherm transformed from type I to type IV.

PHS-1a and PHS-2a were further subjected to pore size expansion using an aqueous solution of tris-(hydroxymethyl)-aminomethane (TRIS) (pH 10.2). The hydrothermal treatment temperature has a significant influence on the pore size expansion. The hydrothermal treatment at 110 and 135 °C for 24 h expanded the pore size of PHS-1a to 63 Å (PHS-1b) and 100 Å (PHS-1c), respectively. But the pore size distributions of the two samples became very wide, especially for the PHS-1c sample that treated at higher temperature. The hydrothermal treatment of sample PHS-2a at 145 and 160 °C also remarkably increased the pore size to 75 and 85 Å, respectively. Unlike the sample of PHS-1b and PHS-1c, the pore size distribution of PHS-2b and PHS-2c still kept typical type IV isotherm with H1 hysteresis loop, which is characteristic of mesoporous materials. The pore size distributions of the two samples remain relatively narrow.

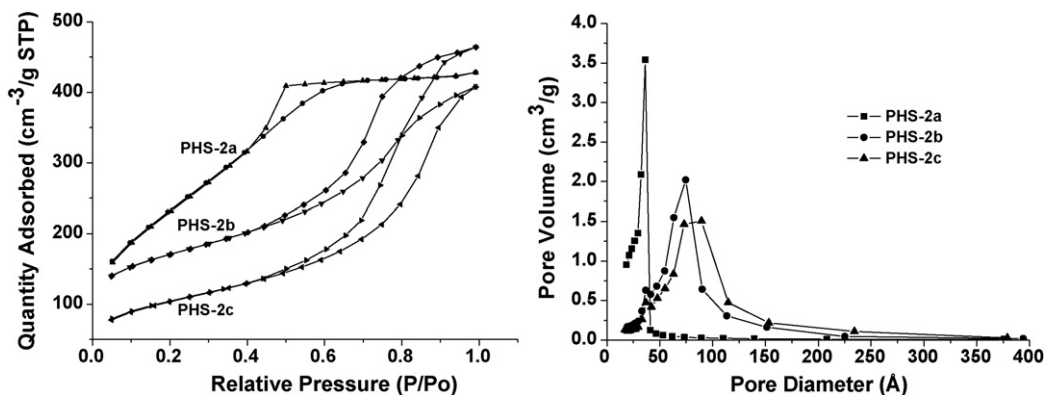


Fig. 4. N_2 adsorption–desorption isotherms and pore size distribution of PHS-2a (removed surfactants after hydrothermal treatment using DMDA at 135 °C), PHS-2b (after hydrothermal treatment using TRIS at 145 °C) and PHS-2c (after hydrothermal treatment using TRIS at 160 °C).

The hydrothermal treatments in the base solution have shown significant pore expansion effect for the phenylene-bridged organosilica spheres. These results consistent with past hydrothermal treatment trends for amorphous silica [42,43] and some other hybrid organosilica materials [44,45], which may be attributed to dissolution of silicates species and reconstruction of pore structure. Compared with mesoporous silica [41,46], the pore sizes of the organosilica materials are relative difficult to expanded, due to the steric effects of phenylene groups incorporated to the pore walls [40,47]. Thus, it is unsurprising that the pore expansion effect was influenced by the content of phenylene groups incorporated into the sample. Comparing with the pore sizes and the pore size distribution curves of sample PHS-2c, PHS-1c exhibits larger pore size and broader pore distribution than PHS-2c, although PHS-2c was treated at higher temperature. On the other hand, the results indicate that with the increasing content of phenylene groups incorporated into the sample, the pore structure becomes more stable, which may lead to more durable under high pH condition when they are used as chromatographic packing.

The SEM images of samples PHS-1c and PHS-2c were shown by Fig. 1(a1) and Fig. 1(b1), respectively. Both of the samples retained high monodispersity and spherical morphology, with the particle diameters before and after hydrothermal treatment unchanged.

3.3. Chemical composition of organosilica materials

The elemental analysis (Table 2) demonstrated that the phenylene groups were successfully incorporated into the pore walls of each sample, and the phenylene group density increased with the increasing of 1,4-BTEB concentration in the initial reaction sol composition increasing.

Table 2
Elemental analysis of as-prepared materials.

Product	C (wt.%)	C ₁₈ density* (μmol/m ²)
PHS-1c	11.8	–
PHS-2c	25.4	–
PHS-C ₁₈	34.6	1.08
S-C ₁₈	17.4	2.42

* C₁₈ density estimated from increased C content.

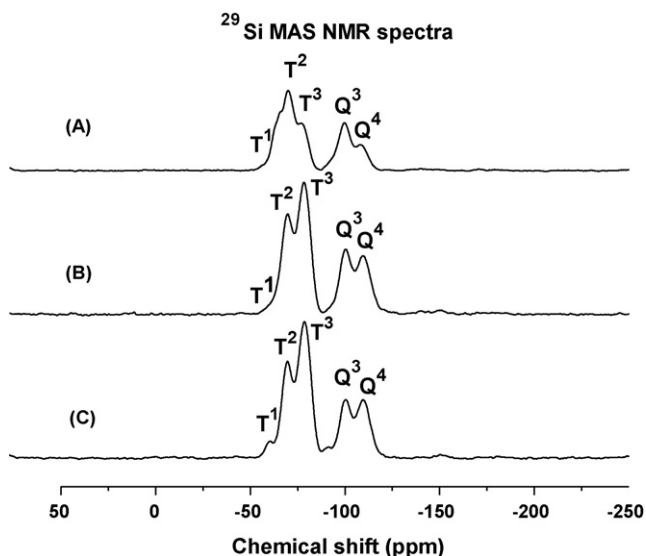


Fig. 5. ²⁹Si CP-MAS NMR for: (A) PHS-2 (before hydrothermal treatment); (B) PHS-2a (after hydrothermal treatment using DMDA at 135 °C); (C) PHS-2c (after hydrothermal treatment using TRIS at 160 °C).

Solid-state ¹³C and ²⁹Si CP-MAS NMR measurements of the PHS-2, PHS-2a and PHS-2c were carried out to investigate the influence of the each hydrothermal treatment process to the chemical environment of phenylene-bridged hybrid organosilicas materials.

The ²⁹Si CP-MAS NMR of samples PHS-2, PHS-2a and PHS-2c were shown in Fig. 5, respectively. The similar signals are given in the spectra. The signals at –62, –70 and –78 ppm were assigned to T¹[SiO(OH)₂SiC], T²[(SiO)₂(OH)SiC] and T³[(SiO)₃SiC], this Tⁿ structural units indicate the appearance of the phenylene-bridged organic groups [48]. The resonances at –100 and –110 ppm are attributed to Q³[(OH)Si(OSi)₃] and Q⁴[Si(OSi)₄], respectively. Here the Qⁿ site was introduced by the hydrolysis of TEOS. Compared three ²⁹Si CP-MAS NMR spectra, it is observed that T³/T² and Q⁴/Q³

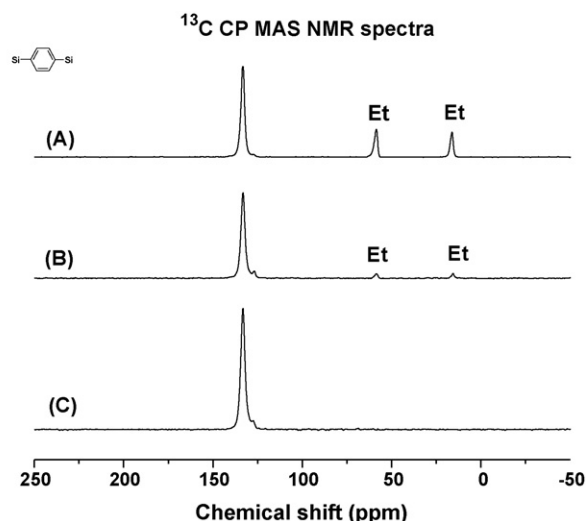


Fig. 6. ¹³C CP-MAS for: (A) PHS-2 (before hydrothermal treatment); (B) PHS-2a (after hydrothermal treatment using DMDA at 135 °C); (C) PHS-2c (after hydrothermal treatment using TRIS at 160 °C).

ratio gradually became higher with each hydrothermal treatment, suggesting that the treatment with DMDA and TRIS leads to silicon species with higher condensation degree [49]. It also demonstrated by the change of ethoxysilyl in the ¹³C CP-MAS NMR spectra.

Fig. 6 shows the ¹³C CP-MAS NMR spectra of the three samples, all the spectra exhibited same distinct peaks with chemical shift of 133 ppm, which are attributed to the carbons in the 1,4-phenylene ring [48,50]. The spectra of the PHS-2 shows the resonances at the 59 and 16 ppm, corresponding to –OCH₂ and –CH₃, respectively, which can be attributed to incomplete hydrolysis of the ethoxysilyl groups of the silsesquioxane [51]. After first hydrothermal treatment, the ethoxysilyl peaks (Fig. 6(B)) were decreased, as well as the peaks removed with hydrothermal treatment in TRIS solution (Fig. 6(C)).

3.4. The chromatographic application

To demonstrate the suitability of this kind of material as HPLC packing materials, the sample PHS-2c (3.0–3.5 μm, 85 Å, 354 m²/g) was further modified by the C₁₈ groups and tested in RP-HPLC. A commercial silica (5 μm, 100 Å, 300 m²/g) based C₁₈ column (S-C₁₈) was also prepared under the same operating conditions to compare with PHS-C₁₈.

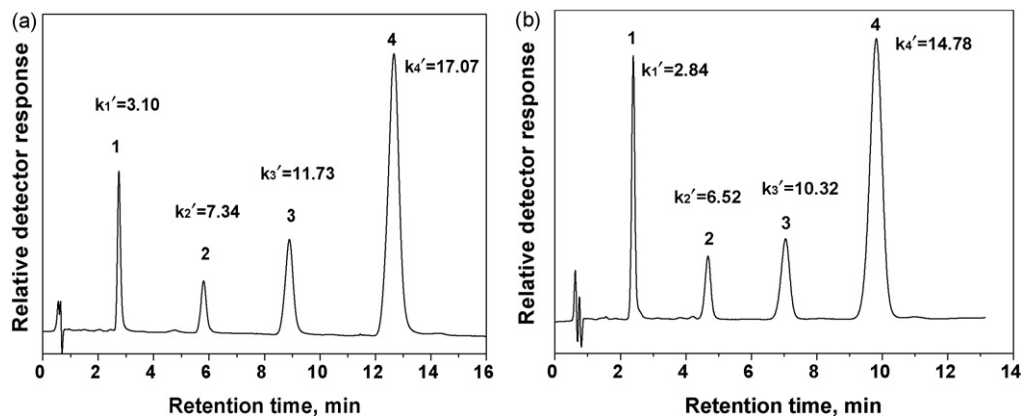


Fig. 7. The chromatograms (a) and (b) obtained with the PHS-C₁₈ column (50 mm × 2.1 mm I.D.) and S-C₁₈ column (50 mm × 2.1 mm I.D.) respectively. Mobile phase: acetonitrile/water (55/45); flow rate: 0.20 mL min⁻¹; 30 °C; UV: 254 nm. Analytes: (1) benzene; (2) naphthalene; (3) biphenyl; (4) phenanthrene.

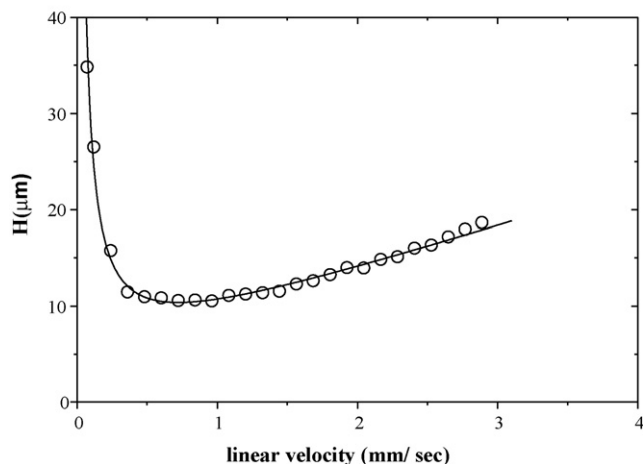


Fig. 8. Plot of theoretical plate height (H) vs. linear velocity. Column: PHS-C₁₈ (2.1 mm × 50 mm); mobile phase: acetonitrile/water (55/45). 30 °C. Test probe: phenanthrene.

The elemental analytical data (shown in Table 2) indicate that C₁₈ have been successfully immobilized onto the phenylene-bridged hybrid organosilica surface. The C₁₈ surface coverages were 1.08 and 2.42 μmol/m² for PHS-C₁₈ and S-C₁₈ calculated from the increasing carbon content, respectively. Primary chromatographic evaluation of PHS-C₁₈ and S-C₁₈ was made using a mixture of aromatic compounds as test probes (Fig. 7). As shown in Fig. 7(a), PHS-C₁₈ has good peak shape and high column efficiency for all the test compounds, especially for phenanthrene, the peaks' symmetry is 1.10 and column efficiency is 95,000 plates m⁻¹. The plotting

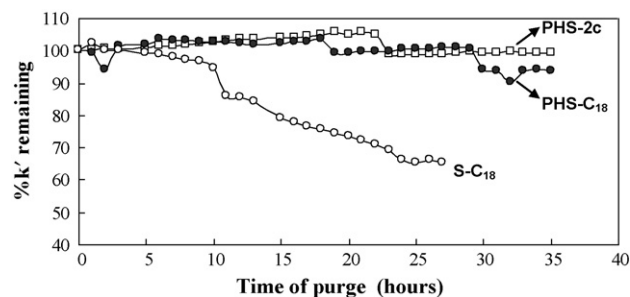


Fig. 9. Loss of retention for columns PHS-C₁₈, PHS-2c, and S-C₁₈ as a function of purge time of 50 mM TEA solution: k' measured for phenanthrene, test conditions are described in Section 2.

HEPT (μm) vs. linear velocity (mm/sec) for column PHS-C₁₈ was depicted in Fig. 8. The column has minimum HETP between 0.5 and 1.0 mm/s. The results demonstrated the suitability of as-prepared phenylene-bridged hybrid organosilicas using for HPLC materials.

The separation efficiencies of PHS-C₁₈ were compared with column S-C₁₈. The chromatogram for separation of aromatic compounds on S-C₁₈ was shown in Fig. 7(b), and the retention factors (k') for aromatic compounds on column PHS-C₁₈ and column S-C₁₈ were summarized in Fig. 7. PHS-C₁₈ packed column exhibited relatively large retention factors for the tested compounds than S-C₁₈, although the coverage of C₁₈ group on PHS-C₁₈ is 2.2 times lower than that on S-C₁₈, which probably due to that the high hydrophobic property of phenylene-bridged hybrid silica supports.

To investigate the chemical stability of unbonded PHS-2c and PHS-C₁₈, an accelerated column aging experiments was investigated by exposing the column to a 50 mM TEA (pH 10, 0.2 mL/min) mobile phase at 50 °C [16,52]. The stability of S-C₁₈ was studied

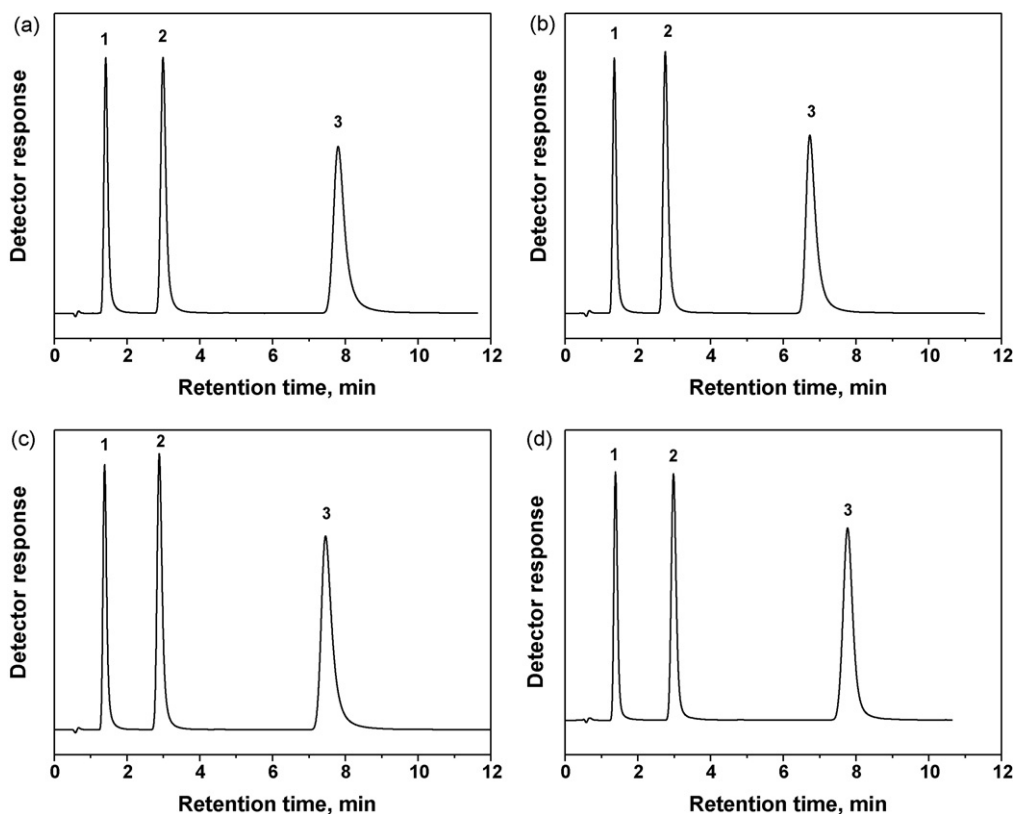


Fig. 10. Chromatograms for three anilines compounds on the PHS-C₁₈ column (2.1 mm × 50 mm) at different mobile phase pH. Conditions: (a) acetonitrile/water (pH 6.0) (40/60, v/v), (b) acetonitrile/0.1% TEAA buffer (pH 4.0) (40/60, v/v), (c) acetonitrile/0.1% TEAA buffer (pH 5.5) (40/60, v/v), (d) acetonitrile/0.1% TEA solution (pH 9.5) (40/60, v/v); flow rate: 0.20 mL/min, UV detector λ = 254 nm. Analytes: (1) aniline; (2) *N*-methylaniline; (3) *N,N*-dimethylaniline.

under same test conditions. Fig. 9 shows plots of relative retention factor measured for phenanthrene versus the TEA solution wash time from accelerated aging tests. For silica based C₁₈ column, the retention factor was maintained greater than 90% only for the first 10 h; after 24h-exposure to the TEA solution, the column efficiency was decreased to about 55% due to the dissolution of the silica particles. In contrast, after the 35 h of exposure to TEA at 50 °C, the PHS-2c column still displayed 100% of their original efficiency, and the PHS-C₁₈ maintained greater than 90% of the initial efficiency. The results demonstrate the better high-pH column stability of PHS-C₁₈ than S-C₁₈, which can be contributed to the high chemical stability of phenylene-bridged hybrid organosilica.

The column PHS-C₁₈ was also evaluated with basic compounds. Fig. 10 shows the separations of three anilines compounds on PHS-C₁₈ at different mobile phase. As shown in Fig. 10(a), three anilines were baseline separated without any addition of the competing amines in the mobile phase. However, the tailing of the *N,N*-dimethylaniline peak (asymmetry factor, 1.70) was obvious, probably due to the unwanted ionic interactions between basic solutes and the unreacted silanol groups on the phenylene-bridged hybrid organosilica support. Fig. 10(b) and (c) shows the separation of the samples at 0.1% triethylamine-acetic acid (TEAA) buffer with pH 4.1 and 5.5, respectively. The retention times of three anilines became shorter, and the peak tailing of the *N,N*-dimethylaniline were still occurring (asymmetry factor, 1.81 and 1.80). When the mobile phase 0.1% triethylamine solution (pH 9.5) were employed, the peak asymmetry of the *N,N*-dimethylaniline was improved to 1.28 (Fig. 10(d)). These phenomena observed can be originated from the case that the basic compounds are in their neutral form under the high pH (pH > 9), and the ionic interactions are reduced. The results indicate that the high pH mobile phases can be used to improve the peak shapes of basic compounds, and they also demonstrate the availability of PHS-C₁₈ column in the separation of basic compounds under the condition of high pH mobile phase.

4. Conclusion

In the study, we have synthesized a series of highly monodisperse 1,4-phenylene-bridged organic/inorganic hybrid silica spheres, with the particle size can be controlled of in the range of 1.5–2.0 and 3.0–3.5 μm, respectively. Moreover, an efficacious strategy based on post-synthesis hydrothermal treatments using DMDA/DDA and TRIS as expander for pore size enlargement of these materials was developed. The resultant sample with sphere sizes between 3 and 3.5 μm and pore diameter up to 85 Å was further modification by C₁₈ and used in HPLC. The preliminary chromatographic results demonstrate the high column efficiency, large retention factor and significant enhancement in column stability at high pH.

Acknowledgment

This work was sponsored by the start-up fund from East China University of Science and Technology, 111 Project (No. B07023) and NSF of China (Grant No. 20601025).

References

[1] J.N. Sogliano, T.R. Floyd, R.A. Harteick, J.M. Dibusso, N.T. Miller, J. Chromatogr. A 443 (1988) 155.

[2] J.J. Kirkland, J.L. Glajch, R.D. Farlee, Anal. Chem. 61 (1989) 2.
 [3] D.V. McCalley, J. Chromatogr. A 769 (1997) 169.
 [4] J.J. Kirkland, J.W. Henderson, J.J. De Stefano, S.M. van Straten, H.A. Claessens, J. Chromatogr. A 762 (1997) 97.
 [5] D.V. McCalley, LC-GC 17 (1999) 440.
 [6] J. Nawrocki, J. Chromatogr. A 779 (1997) 29.
 [7] J.N. Sogliano, R.A. Hartwick, J.M. Dibussolo, N.T. Miller, J. Chromatogr. A 443 (1988) 155.
 [8] J.J. Kirkland, J.J. DeStefano, M.A. Straten, H.A. Claessens, J. Chromatogr. A 762 (1997) 97.
 [9] W.J. Hunks, G.A. Ozin, Chem. Mater. 16 (2004) 5465.
 [10] K.K. Unger, Anal. Chem. 60 (1988) 638.
 [11] G.H. Gu, C.K. Lim, J. Chromatogr. A 515 (1990) 183.
 [12] Y. Mao, B.M. Fung, J. Chromatogr. A 790 (1997) 9.
 [13] M. Kawahara, T. Nakajima, J. Chromatogr. A 515 (1990) 515.
 [14] Y. Inoue, Y. Katsumata, K. Tani, Y. Suzuki, Chromatographia 44 (1997) 538.
 [15] J. Yu, Y.E. Rassi, J. Chromatogr. A 631 (1993) 91.
 [16] K.D. Wyndham, J.E. O'Gara, T.H. Walter, K.H. Glose, N.L. Lawrence, B.A. Alden, G.S. Izzo, C.J. Hudalla, P.C. Iraneta, Anal. Chem. 75 (2003) 6781.
 [17] T. Asefa, M.J. MacLachan, N. Coombs, G.A. Ozin, Nature 402 (1999) 867.
 [18] S. Inagaki, S. Guan, Y. Fukushima, T. Ohsuna, O. Terasaki, J. Am. Chem. Soc. 121 (1999) 9611.
 [19] B.J. Melde, B.T. Holland, C.F. Blanford, A. Stein, Chem. Mater. 11 (1999) 3302.
 [20] W.H. Zhang, B. Daly, J. O'Callaghan, L. Zhang, J.L. Shi, C. Li, M.A. Morris, J.D. Holmes, Chem. Mater. 17 (2005) 6407.
 [21] Y.C. Liang, M. Hanzlik, R. Anwender, J. Mater. Chem. 15 (2005) 3919.
 [22] Y.D. Xia, R. Mokaya, Micropor. Mesopor. Mater. 86 (2005) 231.
 [23] M.P. Kapoor, S. Inagaki, Chem. Mater. 14 (2002) 3509.
 [24] B. Lee, H.M. Luo, C.Y. Yuan, J.S. Lin, S. Dai, Chem. Commun. (2004) 140.
 [25] Y. Goto, S. Inagaki, Chem. Commun. (2002) 2410.
 [26] Q.H. Yang, J. Liu, J. Yang, M.P. Kapoor, S. Inagaki, C. Li, J. Catal. 228 (2004) 265.
 [27] Y. Goto, S. Inagaki, Micropor. Mesopor. Mater. 89 (2006) 103.
 [28] C. Yoshina-Ishii, T. Asefa, N. Coombs, M.J. MacLachlan, G.A. Ozin, Chem. Commun. (1999) 2539.
 [29] M.C. Burleigh, M.A. Markowitz, S. Jayasundera, M.S. Spector, C.W. Thomas, B.P. Gaber, J. Phys. Chem. B 107 (2003) 12628.
 [30] U.D. Neue, T.H. Walter, B.A. Alden, Z. Jiang, R.P. Fisk, J.T. Cook, Am. Lab. 31 (1999) 36.
 [31] Y.F. Cheng, T.H. Walter, Z.L. Lu, P. Iraneta, B.A. Alden, C. Gendreau, U.D. Neue, J.M. Grassi, J.L. Carmody, J.E. O'Gara, R.P. Fisk, LC-GC 18 (2000) 1162.
 [32] V. Rebbin, R. Schmidt, M. Fröba, Angew. Chem. Int. Ed. 45 (2006) 5210.
 [33] Y.P. Zhang, Y. Jin, P.C. Dai, H. Yu, D.H. Yu, Y.X. Ke, X.M. Liang, Anal. Methods 1 (2009) 123.
 [34] J.P. Hanrahan, A. Donovan, M.A. Morris, J.D. Holmes, J. Mater. Chem. 17 (2007) 3881.
 [35] M.F. Ottaviani, M. Cangioti, G. Famigliani, A. Cappiello, J. Phys. Chem. B 110 (2006) 10421.
 [36] J. Nawrocki, C. Dunlap, A. McCormick, P.W. Carr, J. Chromatogr. A 1028 (2004) 1.
 [37] U.D. Neue, E. Serowik, P. Iraneta, B.A. Alden, T.H. Walter, J. Chromatogr. A 849 (1999) 87.
 [38] F. Kleitz, D.N. Liu, G.M. Anilkumar, I.S. Park, L.A. Solovyov, A.N. Shmakov, R. Ryoo, J. Phys. Chem. B 107 (2003) 14296.
 [39] Y.D. Xia, R. Mokaya, J. Phys. Chem. B 110 (2006) 3889.
 [40] X.F. Zhou, S.Z. Qiao, N. Hao, X.L. Wang, C.Z. Yu, L.Z. Wang, D.Y. Zhao, G.Q. Lu, Chem. Mater. 19 (2007) 1870.
 [41] A. Sayari, Angew. Chem. Int. Ed. 39 (2000) 2920.
 [42] J. Ding, C.J. Hudalla, J.T. Cook, D.P. Walsh, C.E. Boissel, P.C. Iraneta, J.E. O'Gara, Chem. Mater. 16 (2004) 670.
 [43] K. Unger, J. Schick-Kalb, B. Straube, Colloid Polym. Sci. 253 (1975) 658.
 [44] Z.P. Jiang, R.P. Fisk, J.E. O'Gara, T.H. Walter, K.D. Wyndham, US Patent, 2007/0243383 A1.
 [45] J.E. O'Gara, M.A. Ashland, US Patent, 2002/0147293 A1.
 [46] A. Sayari, Y. Yang, M. Kruk, M. Jaroniec, J. Phys. Chem. B 103 (1999) 3651.
 [47] M. Kruk, M. Jaroniec, A. Sayari, J. Phys. Chem. B 103 (1999) 4590.
 [48] H. Zhong, G.R. Zhu, J. Yang, P.Y. Wang, Q.H. Yang, Micropor. Mesopor. Mater. 100 (2007) 259.
 [49] G.R. Zhu, H. Zhong, Q.H. Yang, C. Li, Micropor. Mesopor. Mater. 116 (2008) 36.
 [50] S. Inagaki, S. Guan, T. Ohsuna, O. Terasaki, Nature 416 (2002) 304.
 [51] Y.C. Liang, R. Anwender, J. Mater. Chem. 17 (2007) 2506.
 [52] G.R. Zhu, Q.H. Yang, D.M. Jiang, J. Yang, L. Zhang, Y. Li, C. Li, J. Chromatogr. A 1103 (2006) 257.